Altered Intrinsic Brain Activity In Patients With *CSF1R*-Related Leukoencephalopathy

Jingying Wu
Shanghai Sixth Peoples Hospital
Yikang Cao
Jiamusi University
Binyin Li
Shanghai Jiao Tong University Medical School Affiliated Ruijin Hospital
Xize Jia
Hangzhou Normal University Affiliated Hospital
Li Cao (caoli2000@yeah.net)
Shanghai Sixth Peoples Hospital https://orcid.org/0000-0003-1742-9877

Research Article

Keywords: CSF1R-related leukoencephalopathy, amplitude low-frequency fluctuation, regional homogeneity, limbic system, supplementary motor area

Posted Date: July 6th, 2021

DOI: https://doi.org/10.21203/rs.3.rs-618215/v1

Version of Record: A version of this preprint was published at Brain Imaging and Behavior on April 7th, 2022. See the published version at https://doi.org/10.1007/s11682-022-00646-5.

Abstract

Objective: *CSF1R*-related leukoencephalopathy is an adult-onset white matter disease with high disability and mortality, while current diagnostic approaches are prone to misdiagnosis and not sensitive enough for pre-clinical alternations. This study introduced amplitude of low-frequency fluctuations (ALFF) and regional homogeneity (ReHo) based on resting-state functional MRI (rsfMRI) to compare the spontaneous brain activities of patients and healthy controls, aiming to provide early clues for disease onset and enhance our understanding of the disease.

Methods: RsfMRI was performed on 11 patients and 23 healthy controls and preprocessed for calculation of ALFF and ReHo. Permutation tests with threshold free cluster enhancement (number of permutations =5,000) was applied for comparison. Voxels with *P* value<0.05 (family-wise error corrected) and cluster size>10 voxels was considered with significant difference.

Results: Compared to controls, the patient group showed decreased ALFF in right paracentral lobule and precentral gyrus, and increased ALFF in left dorsolateral superior frontal gyrus, left postcentral gyrus, left precentral gyrus, right precuneus, as well as bilateral insula, parahippocampal gyrus, hippocampus, midbrain and cingulate gyrus. Decreased ReHo was found in bilateral supplementary motor area and paracentral lobule of patients, while ReHo increased in right superior occipital gyrus, right precentral gyrus, left angular gyrus, as well as bilateral parahippocampal gyrus, hippocampus, middle occipital gyrus, supramarginal gyrus and extra-nuclear.

Conclusion: These results revealed altered spontaneous brain activities in *CSF1R*-related leukoencephalopathy, especially in limbic system and supplementary motor area, which may serve as an early biomarker for the onset, and shed light on disease mechanisms.

Introduction

The inherited leukoencephalopathy is a heterogeneous group of rare white matter diseases (Kohler, Curiel, & Vanderver, 2018) which affects only 1 in 50,000(Kohler et al., 2018) people. Compared to those young-onset ones, it is even rarer for adult-onset phenotypes such as *CSF1R*-related leukoencephalopathy, making it difficult to collect large samples for relative clinical studies, thus largely limiting the exploration on their mechanisms, diagnosis and treatment. Despite its rarity, studies on *CSF1R*-related leukoencephalopathy are urgently needed, since it mainly affects adults of around 40 years old(Tian et al., 2019) who are usually the main supporters for family, and is associated with high morbidity and mortality that most patients will get bedridden, severe dementia or dying within 4–6 years after diagnosis(Konno et al., 2017; Sundal et al., 2015).

For *CSF1R*-related leukoencephalopathy, early diagnosis is of great significance, because the progression of this fatal disease might be controlled or even slightly reversed if patients receive bone marrow transplantation at the early stage(Eichler et al., 2016; Gelfand et al., 2020; Mochel et al., 2019). However, the incomplete penetrance, which means some carriers may not develop the disease for life, has suggested that *CSF1R* deficiency is not the only factor that determines the early onset of the disease. On the other hand, current diagnosis, which combines genetic analysis with brain structural magnetic resonance imaging (MRI),

featured with asymmetrical periventricular white matters abnormalities on diffusion weighted imaging (DWI) and fluid attenuated inversion recovery (FLAIR) sequence(Bender et al., 2014), is not sensitive enough to detect pre-clinical onset and easily confuse the disease with other disorders with leukoencephalopathy, such as Alzheimer's disease (AD), multiple sclerosis (MS), frontotemporal dementia and cerebral small vessel diseases(Kohler et al., 2018). Therefore, new techniques need to be introduced to improve the early diagnosis of the disease.

Recent studies have shown that the application of single photon emission computered tomography (SPECT) (Daida et al., 2017; Kitani-Morii et al., 2014; Terasawa et al., 2013) and [18F]-fluorodeoxyglucose positron emission tomography (PET)(Kim et al., 2015; Nicholson et al., 2013) has already demonstrated diffuse cortical hypometabolism predominantly in fronto-parietal areas in several cases, indicating the relationship between brain function and *CSF1R*-related leukoencephalopathy. Considering the radioactivity and expensiveness of SPECT and PET, our previous study based on an alternative technique, resting-state functional MRI (rsfMRI), has also revealed some functional abnormalities among patients(Zhan et al., 2020), implying the potential of brain function changes as a contributive biomarker for the early diagnosis of *CSF1R*-related leukoencephalopathy.

In recent years, rsfMRI, as a non-invasive functional imaging technique, has shown its enormous potential in detecting functional abnormalities at an early stage before objective deficits are detectable(Hohenfeld, Werner, & Reetz, 2018), and studying neural mechanisms of neurological dysfunctions (Biswal, 2012), with high acceptance to patients and good reproductivity(Zou et al., 2015). In rsfMRI data analysis, the amplitude of low-frequency fluctuations (ALFF) and regional homogeneity (ReHo) are two commonly calculated local indices(Disner, Marquardt, Mueller, Burton, & Sponheim, 2018; Pan et al., 2017). ALFF is calculated as the mean square root of power spectrum in a low-frequency range (0.01-0.08Hz) at each voxel based on blood oxygenation level-dependent (BOLD) signals(Y. F. Zang et al., 2007). As a promising method for detecting the regional intensity of spontaneous activity, ALFF has been applied in a wide range of brain disorders including AD(X. Liu et al., 2014; Yang et al., 2018), Parkinson's disease (PD)(Hou, Wu, Hallett, Chan, & Wu, 2014; Wang et al., 2020; Yue et al., 2020), MS(Liu et al., 2011), cerebral autosomal dominant arteriopathy with subcortical infarcts and leukoencephalopathy (CADASIL)(Su, Wang, et al., 2019), subcortical ischemic vascular dementia (SIVD)(C. Liu et al., 2014) and moyamoya disease(Lei et al., 2014). On the other hand, ReHo is a measurement for the similarity of the time series of a given cluster. It could reflect local synchronization of spontaneous brain activity and indicate the changes of temporal neuronal activity in specific regional areas. The ReHo method has also been widely used for the investigation of neural activity changes in neurologic diseases, such as AD(Tu et al., 2020; Zhang et al., 2012), PD(Liu et al., 2019; Yue et al., 2020), MS(Wu et al., 2016; Zhu et al., 2020), CADASIL(Orsolini et al., 2020; Su, Ban, et al., 2019) and SIVD(Tu et al., 2020). The combination of ALFF and ReHo might offer us a comprehensive view of regional spontaneous activities in patients with *CSF1R*-related leukoencephalopathy from different dimensions, and provide potential regions of interest for further functional analysis. However, so far, no study has been conducted to explore the characteristics of local brain activity for this disease.

We hypothesize that patients with *CSF1R*-related leukoencephalopathy would exhibit abnormal temporal variability of brain activity compared to healthy controls. 2 resting state methods, ALFF and ReHo were

employed to evaluate the variability of intrinsic brain activities. These might provide early clues for disease onset and enhance our understanding of the disease.

Patients And Methods

Participants

The study was endorsed by the ethics committee of Ruijin Hospital, Shanghai Jiao Tong University School of Medicine, Shanghai, China, and was registered at http://www.chictr.org.cn (No.ChiCTR1800015295). All participants or their guardians provided written informed consent. 17 subjects with *CSF1R*-related leukoencephalopathy and 24 healthy controls were enrolled in the study. Diagnosis of *CSF1R*-related leukoencephalopathy were made by at least two experienced neurologists according to Konno's criteria(Konno et al., 2018). Mini-Mental State Examination (MMSE)-Chinese version and Montreal Cognitive Assessment (MoCA)-Beijing version was used for neuropsychological evaluations, and MRI severity was roughly evaluated according to the score system created by Sundal et al(Sundal et al., 2012).

Imaging Data Acquisition

Imaging data were acquired using a 3.0 Tesla Philips Ingenia MRI scanner with a dStream HeadSpine coil. rsfMRI imaging was carried out using gradient echo planar imaging with the following parameters: 39 continuous axial slices, repetition time (TR) = 2000 ms, echo time (TE) = 30 ms, resolution = 3.5 mm × 3.5 mm × 3.5 mm, thickness = 3.5 with no interslice gap mm, flip angle = 90 degrees, the scan time = approximately 8 minutes. High-resolution T1-weighted images were obtained using three-dimensional brain volume imaging sequences with an acquired voxel size of 1 × 1 × 1 mm^3 as the following parameters: 192 continuous sagittal slices, TR = 7 ms, TE = 3 ms, field of view (FOV) = 256 × 256 mm, flip angle = 7 degrees, slice thickness = 1.0 mm with no interslice gap, matrix size = 256 × 256, and bandwidth = 241 Hz. During the scan, the subjects were placed in a supine position with their head fixed and earplugs worn to reduce noise, and were instructed to lie quietly with their eyes closed but to stay awake without any other tasks.

fMRI Preprocessing

The rsfMRI data were preprocessed using RESTplus V1.24 software(Jia et al., 2019) (http://www.restfmri.net/forum/REST) running in MATLAB2018a(MathWorks, Natick, MA, USA). The preprocessing steps consisted of removal of the first 10 time points for magnetization stabilization, realignment, and spatial normalization. An individual T1-weighted image was co-registered to the mean functional image and then the T1-weighted image was segmented into gray matter (GM), white matter (WM) signal, and cerebrospinal fluid (CSF) signal. The EPI images were spatially normalized to the Montreal Neurological Institute (MNI) space with a resolution of 3 mm x 3 mm x 3 mm. Smoothing was completed using a 6-mm full-width-half-maximum (FWHM) Gaussian kernelto to decrease spatial noise. After removing the linear trend of the time course, nuisance was removed by covariates regression based on Friston-24 head motion(Friston, Williams, Howard, Frackowiak, & Turner, 1996; C. G. Yan et al., 2013) and global mean signal. Scans of 6 patients were excluded because their head motion exceeded 3mm or rotation exceeded 3 degrees in any direction during scanning. Finally, band-pass filter (0.01-0.08Hz) was applied only in ReHo.

ALFF and ReHo Calculation

We use RESTplus V1.24 software to calculate ALFF and ReHo. The calculation of ALFF was based on fast Fourier transform (FFT). Using FFT, each time course was converted to frequency domain and the power spectrum was then obtained. The square root was calculated at each frequency of the power spectrum and then averaged across the filtered band (0.01–0.08 Hz) at each voxel as the ALFF value. For standardization purpose, the ALFF of each voxel was divided by the global mean ALFF value(Y. F. Zang et al., 2007). For ReHo, it was assigned to a given voxel by calculating the Kendall's coefficient of concordance (KCC) of the time series of this voxel with those of its nearest 27 neighboring voxels(Y. Zang, Jiang, Lu, He, & Tian, 2004). To reduce the influence of individual variations in the KCC value, ReHo map normalizations were performed by dividing the KCC among each voxel by the averaged KCC of the whole brain of all the participants in this group. Note that the spatial smoothing (FWHM = 6 mm) was performed after ReHo calculation.

Statistical Analysis

Two-sample *t*-tests were performed to examine the age and education level differences between the two groups and categorical variable like sex was analyzed by Pearson Chi-square test. Data Processing and Analysis for Brain Imaging (DPABI) software (C.-G. Yan, Wang, Zuo, & Zang, 2016) (http://rfmri.org/dpabi) was used for the statistical analyses of the ALFF and ReHo results. A permutation test with a threshold free cluster enhancement (PT TFCE ,number of permutations =5,000) method was used in the two-sample t-tests to compare differences in ALFF and ReHo between patients and controls. Voxels with *P* value <0.05 (family-wise error corrected) and cluster size >10 was considered statistically significant.

Results

Demographic, Clinical and Genetic Findings

Demographic characteristics of 11 patients with *CSF1R*-related leukoencephalopathy (5 males and 6 females; mean age, 39.00 ± 6.34 years) and 23 healthy controls (7 males and 16 females; mean age, 41.61 ± 16.25 years) are demonstrated in Table 1. There was no significant difference found (p > 0.05) in gender, age and education level. Detailed clinical and genetic features of the patient group is shown in Table 2. The average age of onset was 39.45 ± 5.00 years(range 30–47 years) with the average durations of 2.18 ± 1.11 years (range 1–5 years). All those patients suffered from progressive cognition decline, and the average scores of MMSE and MoCA were 19.64 ± 7.20 and 15.50 ± 7.00 respectively. A severity scoring system based on Sundal's study(Sundal et al., 2012) was used to roughly evaluate the MRI changes of each patient, with an average score of 27.09 ± 7.27. 5 novel (c.2498C > G p.T833R, c.834C > A p.C278*, c.2567A > C p.Y856S, c.2473G > C p.E825Q, c.2426A > C p.Y809S) and 4 reported (c.2026C > T p.R676*, c.2381T > C p.I794T, c.2342C > T p.A781V, c.2534T > C p.L845P) mutations of *CSF1R* gene were identified using whole exome sequencing and Sanger sequencing. All the mutations were interpreted to be pathogenic or likely pathogenic following the American College of Medical Genetics and Genomics Standards and Guidelines.

Table 1
The demographics of patients with *CSF1R*-related leukoencephalopathy and healthy controls.

Characteristics	Patients	Controls	P value
Sex(Male/Female)	5/6	7/16	0.4590[a]
Age(years)	39.00 ± 6.34	41.61 ± 16.25	0.6130[b]
Education(years)	10.82 ± 4.49	15.35 ± 4.30	0.0587[b]
[a] Chi-square test; [b]two-sample t-test.			

Table 2
Clinical and genetic characteristics of patients with *CSF1R*-related leukoencephalopathy.

Patient ID	Sex	Onset/Duration (year)	Clinical Manifestations[1]	MRI Scale Score	MMSE/ MoCA	*CSF1R* Mutation[2]	ACMG classification[3]
T4033	F	30/1	CI, PD, BS, Ps	24	14/11	c.2026C > T/p.R676*	Pathogenic
T2980	F	42/1	CI, PD	32	15/NA	c.2026C > T/p.R676*	Pathogenic
T3893	F	35/2	CI, PD, BS, Ps	22	19/15	c.2381T > C/p.I794T	Pathogenic
T4265	M	36/5	CI	10	28/25	c.2381T > C/p.I794T	Pathogenic
T4137	M	45/3	CI, PD, BS, Ps	34	23/15	c.2342C > T/p.A781V	Likely Pathogenic
T4829	M	38/3	CI, Ps	27	23/14	c.2534T > C/p.L845P	Likely Pathogenic
T5555	M	41/2	CI, Ps	35	27/24	c.2498C > G/p.T833R	Likely Pathogenic
T5678	F	47/2	CI, Ps, BS, Ps	35	5/1	c.834C > A/p.C278*	Likely Pathogenic
T5830	F	37/2	CI, Ps, Ps	27	22/21	c.2567A > C/p.Y856S	Likely Pathogenic
T5959	F	46/2	CI, PD	27	13/12	c.2473G > C/p.E825Q	Likely Pathogenic
T6164	M	37/1	CI, PD	25	27/17	c.2426A > C/p.Y809S	Likely Pathogenic

Annotation: [1]CI = cognitive impairment, PD = parkinson's like symptoms, BS = bulbar symptoms like swallow difficulty and/or choking, Ps = psychiatric symptoms. [2] MMSE = Mini Mental State Examination, MoCA = Montreal Cognitive Assessment. [3]Transcript: NM_005211. [4]ACMG = American College of Medical Genetics and Genomics.

Alterations of IBA Changes Between Patients and Healthy Controls

Group Differences in ALFF

As shown in Fig. 1, ALFF decreased in the patient group in right paracentral lobule and precentral gyrus, and increased in left dorsolateral superior frontal gyrus, left postcentral gyrus, left precentral gyrus, right precuneus, as well as bilateral insula, parahippocampal gyrus, hippocampus, midbrain and cingulate gyrus. The significant differences in ALFF between the two groups are shown in Table 3 and Fig.1.

Table 3
Brain regions with significantly differences in ALFF and ReHo between patients with *CSF1R*-related leukoencephalopathy and healthy controls.

Indice	Cluster	Peak (MNI)			Size	Peak intensity
		x	**y**	**z**		
ALFF	**cluster1**	-15	-27	-18	1565	6.5679
	Insula_L				85	
	Parahippocampal_L				56	
	Hippocampus_R				56	
	Hippocampus_L				49	
	Insula_R				26	
	ParaHippocampal_R				23	
	cluster2	0	-39	-27	23	3.8614
	midbrain				18	
	cluster3	-21	54	12	16	5.0088
	Frontal_Sup_L				13	
	cluster4	-36	-27	33	120	4.0456
	Postcentral_L				21	
	Precentral_L				14	
	cluster5	12	6	27	15	4.6241
	Cingulate gyrus				11	
	cluster6	18	-42	54	43	4.9859
	Precuneus_R				9	
	cluster7	9	-24	78	22	-5.2275
	Paracentral_Lobule_R				11	
	Precentral_R				7	
ReHo	**cluster1**	-12	-27	-21	160	5.4193
	Parahippocampal_L				65	
	Hippocampus_L				15	
	cluster2	24	-6	-27	168	4.3835
	ParaHippocampal_R				34	

Hippocampus_R				13	
cluster3	-27	-18	-6	19	4.4146
Extra-nuclear				10	
cluster4	39	-66	27	168	5.4865
Occipital_Mid_R				26	
Occipital_Sup_R				22	
cluster5	-54	-39	30	12	4.3269
SupraMarginal_L				11	
cluster6	48	-30	30	79	5.7666
SupraMarginal_R				52	
cluster7	-36	-75	15	132	6.0441
Occipital_Mid_L				84	
Angular_L				43	
cluster8	45	-6	45	71	4.8706
Precentral_R				67	
cluster9	15	-18	78	253	-5.9087
Supp_Motor_Area_R				53	
Supp_Motor_Area_L				40	
Paracentral_Lobule_R				14	
Paracentral_Lobule_L				13	

Group Differences in ReHo

Compared to the controls, ReHo of the patient group was found decreased in bilateral supplementary motor area and paracentral lobule, and increased in right superior occipital gyrus, right precentral gyrus, left angular gyrus, as well as bilateral parahippocampal gyrus, hippocampus, middle occipital gyrus, supramarginal gyrus and extra-nuclear. Detailed information between the two groups is listed in Table 3 and Fig. 2.

Discussion

CSF1R-related leukoencephalopathy is a rare hereditary white matter disease with high disability and mortality(Konno et al., 2017; Sundal et al., 2015). Current diagnosis that is mainly dependent on gene analysis and structural MRI can easily cause misdiagnosis and is not sensitive enough for pre-clinical alternations(Kohler et al., 2018). Previous studies have illustrated the potential changes in brain function of patients, which might contribute to the early diagnosis(Zhan et al., 2020). Therefore, in this study, we

introduced ALFF and ReHo based on rsfMRI to compare the spontaneous brain activities of patients with *CSF1R*-related leukoencephalopathy and healthy controls. We demonstrated abnormality in extensive regions involving limbic system, sensorimotor area and visual language cortex. These findings may provide insights for the dysfunctional brain patterns of *CSF1R*-related leukoencephalopathy, and may be an early indicator for the disease onset.

The most distinguish pattern in *CSF1R*-related leukoencephalopathy is the increased ALFF and ReHo in limbic system, especially in bilateral parahippocampus gyrus and hippocampus, indicating the increased spontaneous neural activities in these areas. Limbic system is a group of interconnected cortical and subcortical structures that functionally dedicated to the activity of three distinct networks(Catani, Dell'acqua, & Thiebaut de Schotten, 2013). The first network including hippocampal-diencephalic circuit and the parahippocampal-retrosplenical circuit, contributes to memory and spatial orientation(Aggleton, 2008; Vann, Aggleton, & Maguire, 2009) respectively. Altered function of parahippocampus gyrus and hippocampus found in patients with *CSF1R*-related leukoencephalopathy is consistent with the fact that cognitive decline, especially memory loss, is the most common symptom for patients(Konno et al., 2017). Secondly, limbic system also formed the dorsomedial part of default-mode network (DMN)(Raichle et al., 2001), and increased ALFF was also found in parts of this network, including bilateral insula, cingulate gyrus, extra-nuclear and precuneus. The dorsomedial DMN is closely associated with self-referential judgment and recollection of prior experience(Raichle, 2015), thus the alteration of this subnetwork is mostly correlated to neuropsychiatric symptoms such as depression and anxiety(Whitfield-Gabrieli & Ford, 2012; Zhou et al., 2020), which is also the common initial features of *CSF1R*-related leukoencephalopathy. As for the third network, the temporo-amygdala-orbitofrontal network is responsible for the integration of visceral and emotional states with cognition and behavior(Catani et al., 2013), in which there was no significant difference between patients and controls in this study.

The intrinsic brain activities of sensorimotor system are extensively affected, including sensorimotor cortex such as precentral gyrus, postcentral gyrus, paracentral lobule and supplementary motor area (SMA) (Ebbesen & Brecht, 2017), as well as another motor center midbrain, though different area exhibited different pattern according to ALFF and ReHo. Both motor cortex and midbrain have parallel anatomical loops to facilitate or suppress muscle activity, so the abnormality of spontaneous neural activity of these two areas will disturb the control of motor function(Ebbesen & Brecht, 2017), which, in patients with *CSF1R*-related leukoencephalopathy is shown as various motor symptoms such as asymmetric parkinsonism, spasticity and dystonia(Konno et al., 2017). One of the remarkable decreases in ReHo was in SMA. SMA is active before internally generated movement, or even when a motor plan is activated by “object affordance”, that is the facilitation or speeding up of behavioral responses to an object(Nachev, Kennard, & Husain, 2008). Deficits in the SMA is relative to difficulty in gait initiation or execution(Della Sala, Francescani, & Spinnler, 2002; Richard et al., 2017), which resemble the features of gait disturbance in patients with *CSF1R*-related leukoencephalopathy(Konno et al., 2017).

In addition, *CSF1R*-related leukoencephalopathy is related to parietooccipital cortex which is responsible for visuospatial learning, memory and language(Tumati, Martens, de Jong, & Aleman, 2019), including middle occipital gyrus, supramarginal gyrus, angular and superior occipital gyrus. In this disease, abnormality of

these regions might also contribute to cognitive symptoms of patients(Tian et al., 2019). Furthermore, increased ALFF in dorsolateral superior frontal gyrus is also possibly related to execution of cognitive manipulations(Li et al., 2013).

This study had several potential limitations. First of all, limited by the rarity of the disease, the sample size of the study is relatively small, thus further studies with a larger sample are needed. Secondly, we did not investigate the conversion of asymptomatic *CSF1R* mutation carriers to patients in this study, which might help find out the most critical regions during the pathogenesis of the disease. We will try to recruit asymptomatic carriers into our cohort to prospectively follow up their dynamic changes in rsfMRI. In addition, we did not explore the correlation between brain function and gene mutation in *CSF1R*-related leukoencephalopathy, which has been found with potential clinical significance for the treatment and prognosis of AD and PD(Bi, Hu, Wu, & Wang, 2020; Bi, Hu, Xie, & Wu, 2021; Bi, Liu, Xie, Hu, & Jiang, 2020). Besides, it remains unclear about the underlying mechanism of the pathogenesis of *CSF1R*-related leukoencephalopathy. Therefore, it is necessary to apply more methods to analysis the functional abnormality of patients, eventually contributing to early diagnosis of the disease.

Conclusion

In this study, we have investigated the spontaneous brain activity of *CSF1R*-related leukoencephalopathy compared to healthy controls through ALFF and ReHo based on rsfMRI. We have found some unique alternations in the disease in limbic system, sensorimotor system and language areas of the brain. These results suggest a special dysfunctional brain pattern, which may serve as an early biomarker for the detection of the onset of the disease, and indicate the neural circuit mechanisms underlying *CSF1R*-related leukoencephalopathy.

Abbreviations

CSF1R = colony-stimulating factor 1 receptor; MRI = magnetic resonance imaging; DWI = diffusion-weighted imaging; FLAIR = fluid attenuated inversion recovery; AD = Alzheimer's disease; MS = multiple sclerosis; SPECT = single photon emission computered tomography; rsfMRI = resting-state functional MRI; ALFF = amplitude of low-frequency fluctuations; ReHo = regional homogeneity; BOLD = blood oxygenation level-dependent signals; PD = Parkinson's disease; CADASIL = cerebral autosomal dominant arteriopathy with subcortical infarcts and leukoencephalopathy; SIVD = subcortical ischemic vascular dementia; MMSE = Mini-Mental State Examination; MoCA = Montreal Cognitive Assessment; TR = repetition time ; TE = echo time; FOV = field of view; GM = gray matter ; WM = white matter; CSF = cerebrospinal fluid; MNI = Montreal Neurological Institute; FWHM = full-width-half-maximum; FFT = fast Fourier transform; KCC = Kendall's coefficient of concordance; DPABI = Data Processing and Analysis for Brain Imaging; SMA = supplementary motor area.

Declarations

Funding

This work was supported by the grant from National Natural Science Foundation of China (No. 82071258).

Conflicts of interest

None of the authors have a conflict of interest to declare.

Ethics approval

The study was endorsed by the ethics committee of Ruijin Hospital, Shanghai Jiao Tong University School of Medicine, Shanghai, China, and was registered at http://www.chictr.org.cn (No.ChiCTR1800015295).

Consent to participate

All participants or their guardians provided written informed consent.

Consent for publication

All participants or their guardians approved for publication with written consent.

Availability of data and material

All data and material of the study are available from the corresponding author by request.

Code availability

All data were processed with the legal edition of RESTplus V1.24. All code generated or used during the study are available from the corresponding author by request.

Authors' contributions

Author contributions included conception and study design (JW, YC, XJ and LC), data collection or acquisition (JW, BL), statistical analysis (YC and LC), interpretation of results (JW, BL, XJ and LC), drafting the manuscript work or revising it critically for important intellectual content (JW, YC, BL, XJ and LC) and approval of final version to be published and agreement to be accountable for the integrity and accuracy of all aspects of the work (All authors).

References

1. Aggleton, J. P. (2008). EPS Mid-Career Award 2006. Understanding anterograde amnesia: disconnections and hidden lesions. *Q J Exp Psychol (Hove), 61*(10), 1441–1471. doi:10.1080/17470210802215335
2. Bender, B., Klose, U., Lindig, T., Biskup, S., Nagele, T., Schols, L., & Karle, K. N. (2014). Imaging features in conventional MRI, spectroscopy and diffusion weighted images of hereditary diffuse leukoencephalopathy with axonal spheroids (HDLS). *J Neurol*, 261(12), 2351–2359. doi:10.1007/s00415-014-7509-2

3. Bi, X. A., Hu, X., Wu, H., & Wang, Y. (2020). Multimodal Data Analysis of Alzheimer's Disease Based on Clustering Evolutionary Random Forest. *IEEE J Biomed Health Inform*, 24(10), 2973–2983. doi:10.1109/JBHI.2020.2973324
4. Bi, X. A., Hu, X., Xie, Y., & Wu, H. (2021). A novel CERNNE approach for predicting Parkinson's Disease-associated genes and brain regions based on multimodal imaging genetics data. *Med Image Anal*, 67, 101830. doi:10.1016/j.media.2020.101830
5. Bi, X. A., Liu, Y., Xie, Y., Hu, X., & Jiang, Q. (2020). Morbigenous brain region and gene detection with a genetically evolved random neural network cluster approach in late mild cognitive impairment. *Bioinformatics*, 36(8), 2561–2568. doi:10.1093/bioinformatics/btz967
6. Biswal, B. B. (2012). Resting state fMRI: a personal history. *Neuroimage*, 62(2), 938–944. doi:10.1016/j.neuroimage.2012.01.090
7. Catani, M., Dell'acqua, F., & de Thiebaut, M. (2013). A revised limbic system model for memory, emotion and behaviour. *Neurosci Biobehav Rev*, 37(8), 1724–1737. doi:10.1016/j.neubiorev.2013.07.001
8. Daida, K., Nishioka, K., Li, Y., Nakajima, S., Tanaka, R., & Hattori, N. (2017). CSF1R Mutation p.G589R and the Distribution Pattern of Brain Calcification. *Intern Med*, 56(18), 2507–2512. doi:10.2169/internalmedicine.8462-16
9. Della Sala, S., Francescani, A., & Spinnler, H. (2002). Gait apraxia after bilateral supplementary motor area lesion. *J Neurol Neurosurg Psychiatry*, 72(1), 77–85. doi:10.1136/jnnp.72.1.77
10. Disner, S. G., Marquardt, C. A., Mueller, B. A., Burton, P. C., & Sponheim, S. R. (2018). Spontaneous neural activity differences in posttraumatic stress disorder: A quantitative resting-state meta-analysis and fMRI validation. *Hum Brain Mapp*, 39(2), 837–850. doi:10.1002/hbm.23886
11. Ebbesen, C. L., & Brecht, M. (2017). Motor cortex - to act or not to act? *Nat Rev Neurosci*, 18(11), 694–705. doi:10.1038/nrn.2017.119
12. Eichler, F. S., Li, J., Guo, Y., Caruso, P. A., Bjonnes, A. C., Pan, J., & Saxena, R. (2016). CSF1R mosaicism in a family with hereditary diffuse leukoencephalopathy with spheroids. *Brain*, 139(Pt 6), 1666–1672. doi:10.1093/brain/aww066
13. Friston, K. J., Williams, S., Howard, R., Frackowiak, R. S., & Turner, R. (1996). Movement-related effects in fMRI time-series. *Magn Reson Med*, 35(3), 346–355. doi:10.1002/mrm.1910350312
14. Gelfand, J. M., Greenfield, A. L., Barkovich, M., Mendelsohn, B. A., Van Haren, K., Hess, C. P., & Mannis, G. N. (2020). Allogeneic HSCT for adult-onset leukoencephalopathy with spheroids and pigmented glia. *Brain*, 143(2), 503–511. doi:10.1093/brain/awz390
15. Hohenfeld, C., Werner, C. J., & Reetz, K. (2018). Resting-state connectivity in neurodegenerative disorders: Is there potential for an imaging biomarker? *Neuroimage Clin*, 18, 849–870. doi:10.1016/j.nicl.2018.03.013
16. Hou, Y., Wu, X., Hallett, M., Chan, P., & Wu, T. (2014). Frequency-dependent neural activity in Parkinson's disease. *Hum Brain Mapp*, 35(12), 5815–5833. doi:10.1002/hbm.22587
17. Jia, X. Z., Wang, J., Sun, H. Y., Zhang, H., Liao, W., Wang, Z., & Zang, Y. F. (2019). RESTplus: an improved toolkit for resting-state functional magnetic resonance imaging data processing. *Science Bulletin*, 64(14), 953–954. doi:10.1016/j.scib.2019.05.008

18. Kim, E. J., Shin, J. H., Lee, J. H., Kim, J. H., Na, D. L., Suh, Y. L., & Huh, G. Y. (2015). Adult-onset leukoencephalopathy with axonal spheroids and pigmented glia linked CSF1R mutation: Report of four Korean cases. *J Neurol Sci*, 349(1–2), 232–238. doi:10.1016/j.jns.2014.12.021
19. Kitani-Morii, F., Kasai, T., Tomonaga, K., Saito, K., Mizuta, I., Yoshioka, A., & Mizuno, T. (2014). Hereditary diffuse leukoencephalopathy with spheroids characterized by spastic hemiplegia preceding mental impairment. *Intern Med*, 53(12), 1377–1380. doi:10.2169/internalmedicine.53.1932
20. Kohler, W., Curiel, J., & Vanderver, A. (2018). Adulthood leukodystrophies. *Nat Rev Neurol*, 14(2), 94–105. doi:10.1038/nrneurol.2017.175
21. Konno, T., Yoshida, K., Mizuno, T., Kawarai, T., Tada, M., Nozaki, H., & Ikeuchi, T. (2017). Clinical and genetic characterization of adult-onset leukoencephalopathy with axonal spheroids and pigmented glia associated with CSF1R mutation. *Eur J Neurol*, 24(1), 37–45. doi:10.1111/ene.13125
22. Konno, T., Yoshida, K., Mizuta, I., Mizuno, T., Kawarai, T., Tada, M., & Ikeuchi, T. (2018). Diagnostic criteria for adult-onset leukoencephalopathy with axonal spheroids and pigmented glia due to CSF1R mutation. *Eur J Neurol*, 25(1), 142–147. doi:10.1111/ene.13464
23. Lei, Y., Li, Y., Ni, W., Jiang, H., Yang, Z., Guo, Q., & Mao, Y. (2014). Spontaneous brain activity in adult patients with moyamoya disease: a resting-state fMRI study. *Brain Res*, 1546, 27–33. doi:10.1016/j.brainres.2013.12.022
24. Li, W., Qin, W., Liu, H., Fan, L., Wang, J., Jiang, T., & Yu, C. (2013). Subregions of the human superior frontal gyrus and their connections. *Neuroimage*, 78, 46–58. doi:10.1016/j.neuroimage.2013.04.011
25. Liu, C., Li, C., Yin, X., Yang, J., Zhou, D., Gui, L., & Wang, J. (2014). Abnormal intrinsic brain activity patterns in patients with subcortical ischemic vascular dementia. *PLoS One*, 9(2), e87880. doi:10.1371/journal.pone.0087880
26. Liu, X., Wang, S., Zhang, X., Wang, Z., Tian, X., & He, Y. (2014). Abnormal amplitude of low-frequency fluctuations of intrinsic brain activity in Alzheimer's disease. *J Alzheimers Dis*, 40(2), 387–397. doi:10.3233/JAD-131322
27. Liu, Y., Li, M., Chen, H., Wei, X., Hu, G., Yu, S., & Xie, Y. (2019). Alterations of Regional Homogeneity in Parkinson's Disease Patients With Freezing of Gait: A Resting-State fMRI Study. *Front Aging Neurosci*, 11, 276. doi:10.3389/fnagi.2019.00276
28. Liu, Y., Liang, P., Duan, Y., Jia, X., Yu, C., Zhang, M., & Li, K. (2011). Brain plasticity in relapsing-remitting multiple sclerosis: evidence from resting-state fMRI. *J Neurol Sci*, 304(1–2), 127–131. doi:10.1016/j.jns.2011.01.023
29. Mochel, F., Delorme, C., Czernecki, V., Froger, J., Cormier, F., Ellie, E., & Nguyen, S. (2019). Haematopoietic stem cell transplantation in CSF1R-related adult-onset leukoencephalopathy with axonal spheroids and pigmented glia. *J Neurol Neurosurg Psychiatry*, 90(12), 1375–1376. doi:10.1136/jnnp-2019-320701
30. Nachev, P., Kennard, C., & Husain, M. (2008). Functional role of the supplementary and pre-supplementary motor areas. *Nat Rev Neurosci*, 9(11), 856–869. doi:10.1038/nrn2478
31. Nicholson, A. M., Baker, M. C., Finch, N. A., Rutherford, N. J., Wider, C., Graff-Radford, N. R., & Rademakers, R. (2013). CSF1R mutations link POLD and HDLS as a single disease entity. *Neurology*, 80(11), 1033–1040. doi:10.1212/WNL.0b013e31828726a7

32. Orsolini, S., Marzi, C., Gavazzi, G., Bianchi, A., Salvadori, E., Giannelli, M., & Diciotti, S. (2020). Altered Regional Brain Homogeneity of BOLD Signal in CADASIL: A Resting State fMRI Study. *J Neuroimaging*. doi:10.1111/jon.12821
33. Pan, P., Zhu, L., Yu, T., Shi, H., Zhang, B., Qin, R., & Xu, Y. (2017). Aberrant spontaneous low-frequency brain activity in amnestic mild cognitive impairment: A meta-analysis of resting-state fMRI studies. *Ageing Res Rev*, 35, 12–21. doi:10.1016/j.arr.2016.12.001
34. Raichle, M. E. (2015). The brain's default mode network. *Annu Rev Neurosci*, 38, 433–447. doi:10.1146/annurev-neuro-071013-014030
35. Raichle, M. E., MacLeod, A. M., Snyder, A. Z., Powers, W. J., Gusnard, D. A., & Shulman, G. L. (2001). A default mode of brain function. *Proc Natl Acad Sci U S A*, 98(2), 676–682. doi:10.1073/pnas.98.2.676
36. Richard, A., Van Hamme, A., Drevelle, X., Golmard, J. L., Meunier, S., & Welter, M. L. (2017). Contribution of the supplementary motor area and the cerebellum to the anticipatory postural adjustments and execution phases of human gait initiation. *Neuroscience*, 358, 181–189. doi:10.1016/j.neuroscience.2017.06.047
37. Su, J., Ban, S., Wang, M., Hua, F., Wang, L., Cheng, X., & Liu, J. (2019). Reduced resting-state brain functional network connectivity and poor regional homogeneity in patients with CADASIL. *J Headache Pain*, 20(1), 103. doi:10.1186/s10194-019-1052-6
38. Su, J., Wang, M., Ban, S., Wang, L., Cheng, X., Hua, F., & Liu, J. (2019). Relationship between changes in resting-state spontaneous brain activity and cognitive impairment in patients with CADASIL. *J Headache Pain*, 20(1), 36. doi:10.1186/s10194-019-0982-3
39. Sundal, C., Baker, M., Karrenbauer, V., Gustavsen, M., Bedri, S., Glaser, A., & Andersen, O. (2015). Hereditary diffuse leukoencephalopathy with spheroids with phenotype of primary progressive multiple sclerosis. *Eur J Neurol*, 22(2), 328–333. doi:10.1111/ene.12572
40. Sundal, C., Van Gerpen, J. A., Nicholson, A. M., Wider, C., Shuster, E. A., Aasly, J., & Wszolek, Z. K. (2012). MRI characteristics and scoring in HDLS due to CSF1R gene mutations. *Neurology*, 79(6), 566–574. doi:10.1212/WNL.0b013e318263575a
41. Terasawa, Y., Osaki, Y., Kawarai, T., Sugimoto, T., Orlacchio, A., Abe, T., & Kaji, R. (2013). Increasing and persistent DWI changes in a patient with hereditary diffuse leukoencephalopathy with spheroids. *J Neurol Sci*, 335(1–2), 213–215. doi:10.1016/j.jns.2013.08.027
42. Tian, W. T., Zhan, F. X., Liu, Q., Luan, X. H., Zhang, C., Shang, L., & Cao, L. (2019). Clinicopathologic characterization and abnormal autophagy of CSF1R-related leukoencephalopathy. *Transl Neurodegener*, 8, 32. doi:10.1186/s40035-019-0171-y
43. Tu, M. C., Hsu, Y. H., Yang, J. J., Huang, W. H., Deng, J. F., Lin, S. Y., & Kuo, L. W. (2020). Attention and Functional Connectivity Among Patients With Early-Stage Subcortical Ischemic Vascular Disease and Alzheimer's Disease. *Front Aging Neurosci*, 12, 239. doi:10.3389/fnagi.2020.00239
44. Tumati, S., Martens, S., de Jong, B. M., & Aleman, A. (2019). Lateral parietal cortex in the generation of behavior: Implications for apathy. *Prog Neurobiol*, 175, 20–34. doi:10.1016/j.pneurobio.2018.12.003
45. Vann, S. D., Aggleton, J. P., & Maguire, E. A. (2009). What does the retrosplenial cortex do? *Nat Rev Neurosci*, 10(11), 792–802. doi:10.1038/nrn2733

46. Wang, Z., Liu, Y., Ruan, X., Li, Y., Li, E., Zhang, G., & Wei, X. (2020). Aberrant Amplitude of Low-Frequency Fluctuations in Different Frequency Bands in Patients With Parkinson's Disease. *Front Aging Neurosci*, 12, 576682. doi:10.3389/fnagi.2020.576682
47. Whitfield-Gabrieli, S., & Ford, J. M. (2012). Default mode network activity and connectivity in psychopathology. *Annu Rev Clin Psychol*, 8, 49–76. doi:10.1146/annurev-clinpsy-032511-143049
48. Wu, L., Zhang, Y., Zhou, F., Gao, L., He, L., Zeng, X., & Gong, H. (2016). Altered intra- and interregional synchronization in relapsing-remitting multiple sclerosis: a resting-state fMRI study. *Neuropsychiatr Dis Treat*, 12, 853–862. doi:10.2147/NDT.S98962
49. Yan, C. G., Wang, X. D., Zuo, X. N., & Zang, Y. F. (2016). DPABI: Data Processing & Analysis for (Resting-State) Brain Imaging. *Neuroinformatics*, 14(3), 339–351. doi:10.1007/s12021-016-9299-4
50. Yan, C. G., Cheung, B., Kelly, C., Colcombe, S., Craddock, R. C., Di Martino, A., & Milham, M. P. (2013). A comprehensive assessment of regional variation in the impact of head micromovements on functional connectomics. *Neuroimage*, 76, 183–201. doi:10.1016/j.neuroimage.2013.03.004
51. Yang, L., Yan, Y., Wang, Y., Hu, X., Lu, J., Chan, P., & Han, Y. (2018). Gradual Disturbances of the Amplitude of Low-Frequency Fluctuations (ALFF) and Fractional ALFF in Alzheimer Spectrum. *Front Neurosci*, 12, 975. doi:10.3389/fnins.2018.00975
52. Yue, Y., Jiang, Y., Shen, T., Pu, J., Lai, H. Y., & Zhang, B. (2020). ALFF and ReHo Mapping Reveals Different Functional Patterns in Early- and Late-Onset Parkinson's Disease. *Front Neurosci*, 14, 141. doi:10.3389/fnins.2020.00141
53. Zang, Y., Jiang, T., Lu, Y., He, Y., & Tian, L. (2004). Regional homogeneity approach to fMRI data analysis. *Neuroimage*, 22(1), 394–400. doi:10.1016/j.neuroimage.2003.12.030
54. Zang, Y. F., He, Y., Zhu, C. Z., Cao, Q. J., Sui, M. Q., Liang, M., & Wang, Y. F. (2007). Altered baseline brain activity in children with ADHD revealed by resting-state functional MRI. *Brain Dev*, 29(2), 83–91. doi:10.1016/j.braindev.2006.07.002
55. Zhan, F. X., Zhu, Z. Y., Liu, Q., Zhou, H. Y., Luan, X. H., Huang, X. J., & Cao, L. (2020). Altered structural and functional connectivity in CSF1R-related leukoencephalopathy. *Brain Imaging Behav*. doi:10.1007/s11682-020-00360-0
56. Zhang, Z., Liu, Y., Jiang, T., Zhou, B., An, N., Dai, H., & Zhang, X. (2012). Altered spontaneous activity in Alzheimer's disease and mild cognitive impairment revealed by Regional Homogeneity. *Neuroimage*, 59(2), 1429–1440. doi:10.1016/j.neuroimage.2011.08.049
57. Zhou, H. X., Chen, X., Shen, Y. Q., Li, L., Chen, N. X., Zhu, Z. C., & Yan, C. G. (2020). Rumination and the default mode network: Meta-analysis of brain imaging studies and implications for depression. *Neuroimage*, 206, 116287. doi:10.1016/j.neuroimage.2019.116287
58. Zhu, Y., Huang, M., Zhao, Y., Pei, Y., Wang, Y., Wang, L., & Zeng, X. (2020). Local functional connectivity of patients with acute and remitting multiple sclerosis: A Kendall's coefficient of concordance- and coherence-regional homogeneity study. *Medicine (Baltimore)*, 99(43), e22860. doi:10.1097/MD.0000000000022860
59. Zou, Q., Miao, X., Liu, D., Wang, D. J., Zhuo, Y., & Gao, J. H. (2015). Reliability comparison of spontaneous brain activities between BOLD and CBF contrasts in eyes-open and eyes-closed resting states.

Neuroimage, 121, 91–105. doi:10.1016/j.neuroimage.2015.07.044

Figures

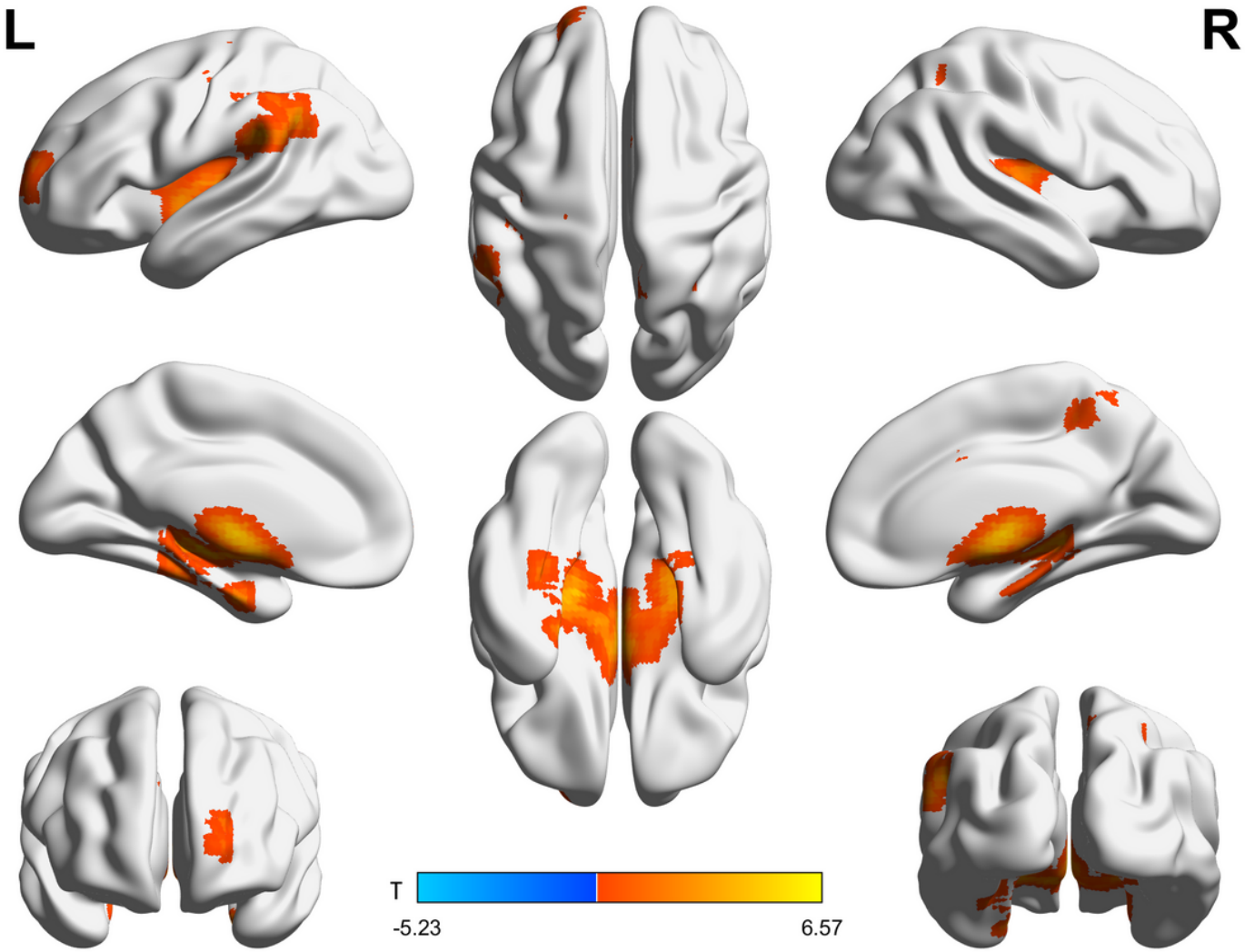

Figure 1

Changes of ALFF in patients with CSF1R-related leukoencephalopathy. The patients group showed increased ALFF in left dorsolateral superior frontal gyrus, left postcentral gyrus, left precentral gyrus, right precuneus, as well as bilateral insula, parahippocampal gyrus, hippocampus, midbrain and cingulate gyrus, and the ALFF value decreased in right paracentral lobule and precentral gyrus (P<0.05, family-wise error corrected). The t-values are color-coded.

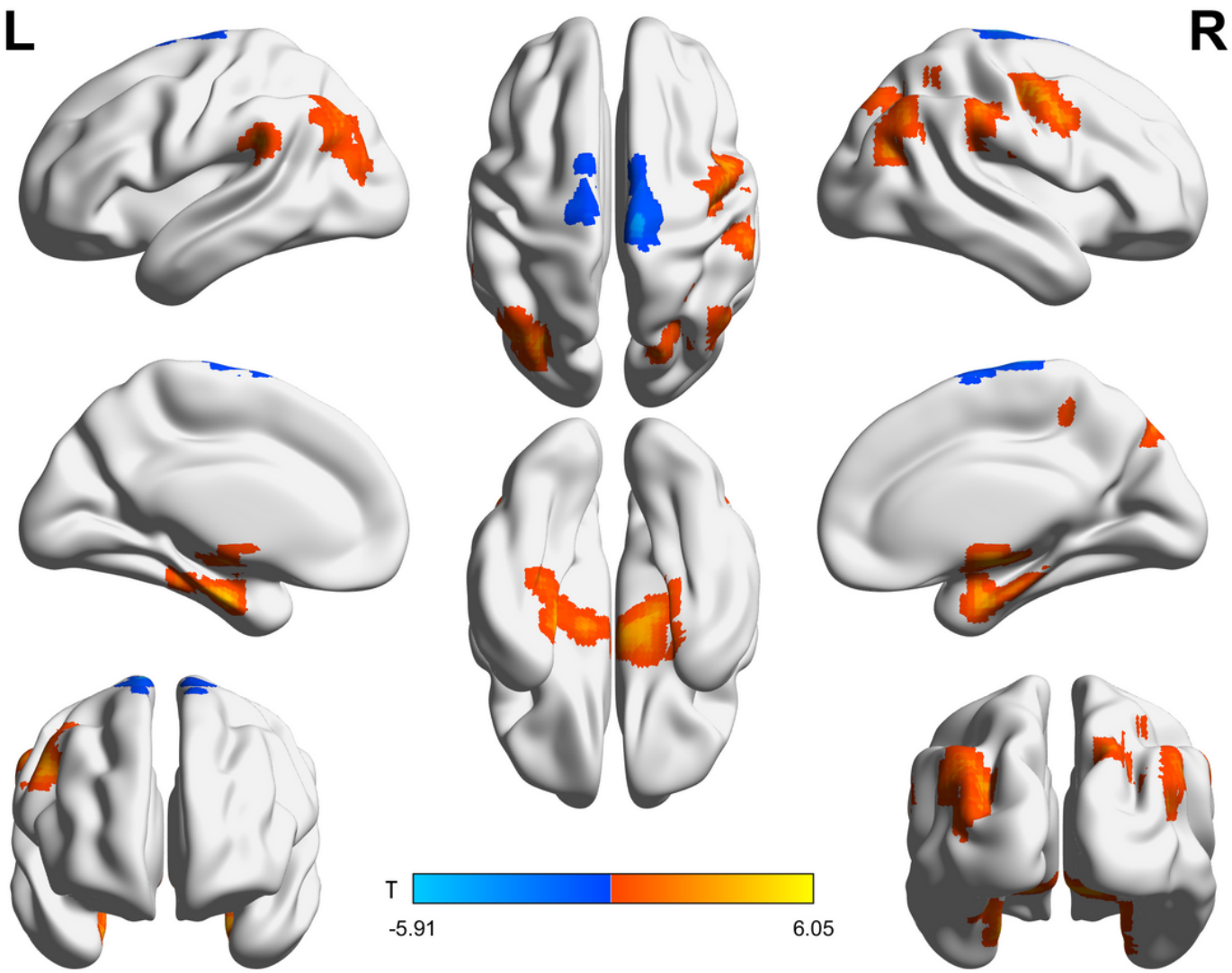

Figure 2

Changes of ReHo in patients with CSF1R-related leukoencephalopathy. The ReHo value of the patient group increased in right superior occipital gyrus, right precentral gyrus, left angular gyrus, as well as bilateral parahippocampal gyrus, hippocasSmpus, middle occipital gyrus, supramarginal gyrus and extra-nuclear, while decreased in bilateral supplementary motor area and paracentral lobule (P<0.05, family-wise error corrected). The t-values are color-coded.

Supplementary Files

This is a list of supplementary files associated with this preprint. Click to download.

- BIBChecklist.docx